JOURNAL OF MATERIALS SCIENCE 16 (1981) 2387–2397

Thermal decomposition of ferrous oxalate dihydrate studied by direct current electrical conductivity measurements

K. S. RANE, A. K. NIKUMBH, A. J. MUKHEDKAR
University Department of Chemistry, Ganeshkhind, Pune 411 007, India

The feasibility of the use of direct current electrical conductivity, σ, measurements in the study of solid-state reactions involved in the synthesis of γ-Fe_2O_3 from ferrous oxalate dihydrate has been reported. The study has been carried out in static air, dynamic air, dry nitrogen and dynamic air + water vapour environments. The conductivity data determined in static air are quite complex; nevertheless, the formation of Fe_3O_4 and α-Fe_2O_3 with the probable intermediate formation of γ-Fe_2O_3 has been indicated. In dry nitrogen the step corresponding to dehydration is well resolved in the temperature region 145–220° C; the formation of FeO and Fe_3O_4 is also well characterized. In dry dynamic air the reaction further proceeds to the formation of α-Fe_2O_3. In dynamic air containing water vapour there are definite indications of the formation of γ-Fe_2O_3 prior to the formation of α-Fe_2O_3. Definite experimental conditions have been determined for the formation of γ-Fe_2O_3 in dynamic air containing water vapour. The conductivity measurements have been supplemented with infra-red spectroscopy and X-ray diffraction pattern measurements. The electrical conductivity measurements were found to give additional information on the solid-state reaction to that obtained from conventional thermal analytical techniques (such as differential thermal, thermogravimetric and differential thermogravimetric analyses). γFe_2O_3, obtained from the decomposition of $FeC_2O_4 \cdot 2H_2O$ in dynamic air + water was found to have a coercive force of 3.142 A m^{-1}, a saturation magnetization value of 7.1 T kg^{-1} and a ratio of remanence to saturation magnetization of 0.64.

1. Introduction

Maghemite (γ-Fe_2O_3) is an important magnetic material. Among the various methods for preparing γ-Fe_2O_3, the thermal decomposition of ferrous oxalate dihydrate, $FeC_2O_4 \cdot 2H_2O$, would seem to be promising as crystals of the oxalate complex can be easily obtained in an acicular form. The thermal decomposition of $FeC_2O_4 \cdot 2H_2O$ under normal atmospheric conditions gives the more stable crystalline modification of ferric oxide, namely α-Fe_2O_3. The thermal decomposition in air of $FeC_2O_4 \cdot 2H_2O$ containing traces of moisture under the ambient conditions of its own gaseous products at about 300° C yields mainly γ-Fe_2O_3. However, X-ray data of the sample [1] thus synthesised, show weak lines corresponding to α-Fe_2O_3 superimposed on the pattern of γ-Fe_2O_3. Since using this procedure it is not possible to specify the exact conditions of atmosphere used during the synthesis of γ-Fe_2O_3, a study of the thermal decomposition of $FeC_2O_4 \cdot 2H_2O$ under a controlled atmosphere has been undertaken in the present work.

In the literature, thermogravimetry (TG), differential thermal analysis (DTA) and differential thermogravimetry (DTG) data, supplemented with X-ray diffraction data, have been used to study the progress of the thermal decomposition of $FeC_2O_4 \cdot 2H_2O$ [1, 3]. In such a study it was not possible to characterize the temperature at which γ-Fe_2O_3 could be obtained in air since a broad exothermic peak constituted the reactions

0022–2461/81/092387–11$03.10/0

corresponding to the decomposition of FeC_2O_4 to FeO and Fe_3O_4, and the further transformation to α-Fe_2O_3 through γ-Fe_2O_3. It would therefore be profitable to use another technique which may help to differentiate these various steps of the solid-state reactions leading to the formation of α-Fe_2O_3. The present work investigates the feasibility of the measurement of the direct current (d.c.) electrical conductivity as a probe for the study of the progress of the thermal decomposition of $FeC_2O_4 \cdot 2H_2O$. Interest has recently been shown in the use of this technique for the study of solid-state decomposition reactions [4].

2. Experimental procedure

2.1. Sample preparation

Ferrous oxalate dihydrate was prepared using the usual procedure, that used in [2]. Wet chemical analysis of the oxalate gave Fe: 30.6 wt%; C_2O_4: 48.8 wt%; H_2O: 20.0 wt%. calc. Calculated contents for the oxalate are Fe: 31.0 wt%; C_2O_4: 48.9 wt%; H_2O: 20.0 wt%. For the study of the decomposition of oxalate in dynamic air, an air compressor was used. The air-flow was maintained between 60 and 65 ml min^{-1}. In the decomposition study in dynamic air + water vapour the air was bubbled (at a rate of 60 to 65 ml min^{-1}) through water in a flask maintained, using a thermostat, at a temperature of 60–61° C.

2.2. X-ray diffraction studies

The products of decomposition of $FeC_2O_4 \cdot 2H_2O$ were analysed by X-ray powder diffraction techniques using Mo$K\alpha$ radiation (wavelength $\lambda =$ 0.709 Å, using a zirconium filter) on a PW 1730 Philips X-ray diffractometer. The experimentaly observed d-spacing values and relative intensities were compared with those reported in the ASTM File.

2.3. Infra-red spectroscopy study

Infra-red spectra were recorded on a Perkin Elmer Model 337 spectrophotometer using nujol mull.

2.4. Magnetic hysteresis measurements

The hysteresis studies were made using an alternating electromagnet-type hysteresis loop tracer similar to that described by Likhite *et al.* [5]. The instrument was calibrated for the magnetization measurements using pure nickel (99.9 % pure) as the standard.

2.5. Direct current electrical conductivity measurements

The direct current (d.c.) electrical conductivity, σ, measurement was measured by the two-probe method. The sample, in the form of a pellet weight: 0.90 g; diameter 10 mm; thickness: 3.5 ± 0.2 mm; pressure at which the pellet was formed: 1.8×10^2 kg cm^{-2} was pressed between two spring-loaded platinum electrodes and the resistivity was measured in the usual manner by measuring the difference in potential between the electrodes for a known current across the specimen. The potential developed between the potential probes was measured using a Philips PP 9004 microvoltmeter. For direct measurement of resistance the Philips GM 6009 ohmmeter was used. The specific conductivity was obtained by taking into consideration the dimensions of probe and sample. No attempt was made to determine accurately the absolute value of the resistivity since it was the temperature variation of resistivity that was of interest in the study.

The conductivity cell was designed so that different atmospheres could be used. The cell was kept in a tubular furnace whose temperature was controlled within ± 1° C. A precalibrated Chromel–Alumel thermocouple was used for sensing the temperature (± 0.1° C). Philips PP 9004 microvoltmeter was used to read the potential developed between the hot zone and the cold zone (ice water).

For the decomposition study, the heating rate of about 3° C min^{-1} was manually controlled with a predetermined operation of the variac. Precautions were taken to maintain a constant rate of heating. (It may be noted here than no localized red glow, as has been reported in [1], could be detected during the reactions in the controlled dynamic atmospheres.) The conductivity data are presented as $\log \sigma$ against $10^3 T^{-1}$ (K^{-1}) in Figs 1 to 5. The data were determined using four different pellets of the same sample, and it was observed that the pattern of the σ–T^{-1} plots were reproducible to within ± 1° C.

3. Results and discussion

The temperature variation of electrical conductivity of $FeC_2O_4 \cdot 2H_2O$ determined in normal static air (see Fig. 1) shows the following characteristics. The conductivity of the pure complex in air at room temperature (27° C) is low (about 10^{-11} ohm^{-1} cm^{-1}). The specific conductivity,

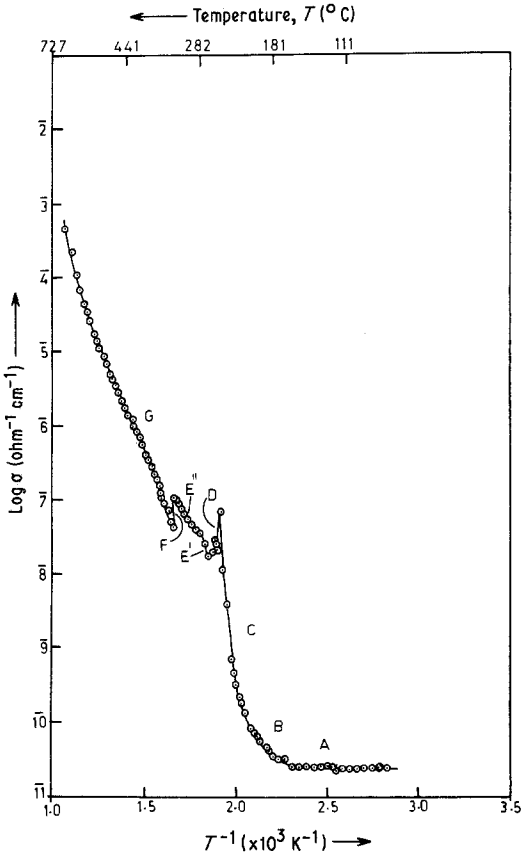

Figure 1 Plot of log σ against T^{-1} of $FeC_2O_4 \cdot 2H_2O$ during decomposition in static air.

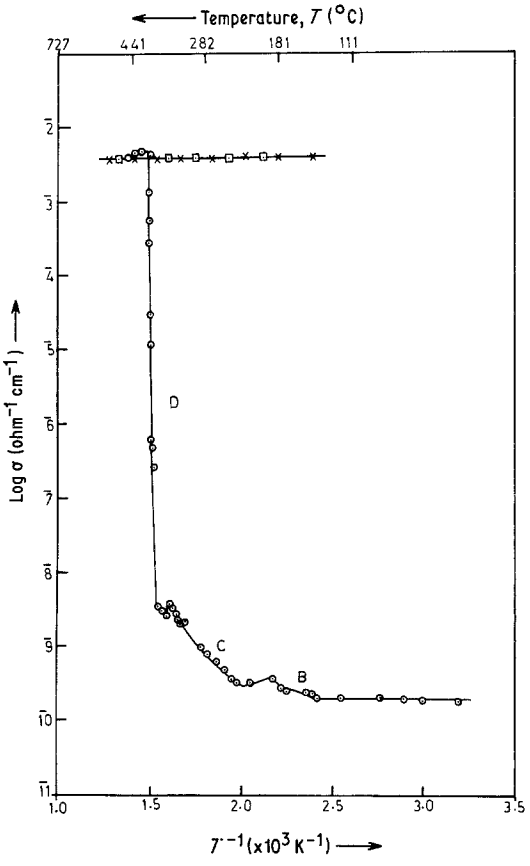

Figure 2 Plot of log σ against T^{-1} of FeC_2O_4 during decomposition in dynamic dry nitrogen. ⊙During composition; ⊡ cooling cycle for Fe_3O_4; × heating cycle for Fe_3O_4.

σ, does not show much change with variation of temperature from 27 to 161° C (A in Fig. 1). There is a steady increase in σ between 161 and 207° C (B in Fig. 1). A steep increase in σ is observed at 207° C giving a maximum at 247° C (C in Fig. 1). There then is a linear decrease in σ between 247 and 265° C (D in Fig. 1) and, again, σ starts rising from 265 to 333° C giving a definite shoulder at 282° C (E′–E″ in Fig. 1). A sudden decrease in σ at 322° C (F in Fig. 1) is then followed by a region of roughly linear increase in log σ with T beginning at 329° C (G in Fig. 1).

A comparison of conventional thermal analysis [1–3] in air with conductivity analysis in air of $FeC_2O_4 \cdot 2H_2O$ shows that the conductivity analysis gives a much more detailed view of the decomposition process. TG shows a continuous mass loss between 170 and 270° C. DTA gives an endothermic peak at about 190° C corresponding to the dehydration of the dihydrate complex, a broad exothermic peak (at about 240° C) between 215 and 290° C corresponding to the oxidative decomposition of FeC_2O_4 to the poorly-crystallized α-Fe_2O_3, and a weak ill-characterised exothermic peak at about 360° C which has been tentatively assigned to a transformation of the poorly-crystallized α-Fe_2O_3 to the crystalline α-Fe_2O_3 [1]. It should be noted here that there are inconsistencies in the results of TG, DTG and DTA of $FeC_2O_4 \cdot 2H_2O$ reported by different workers [1–3].

It is well recognised that the thermal decomposition of $FeC_2O_4 \cdot 2H_2O$ does not directly yield α-Fe_2O_3: it proceeds through the formation of FeO, Fe_3O_4 and γ-Fe_2O_3. These additional steps are not resolvable from conventional TG, DTG and DTA curves.

The analysis of the log σ against T^{-1} plot must give due consideration to the physical factors involved in transforming a compound (formed during a chemical reaction) in the amorphous phase or fusion layers to large crystallites through the probable transformations, such as the formation of a fine network of grain boundaries and subsequent consolidation, and the formation of

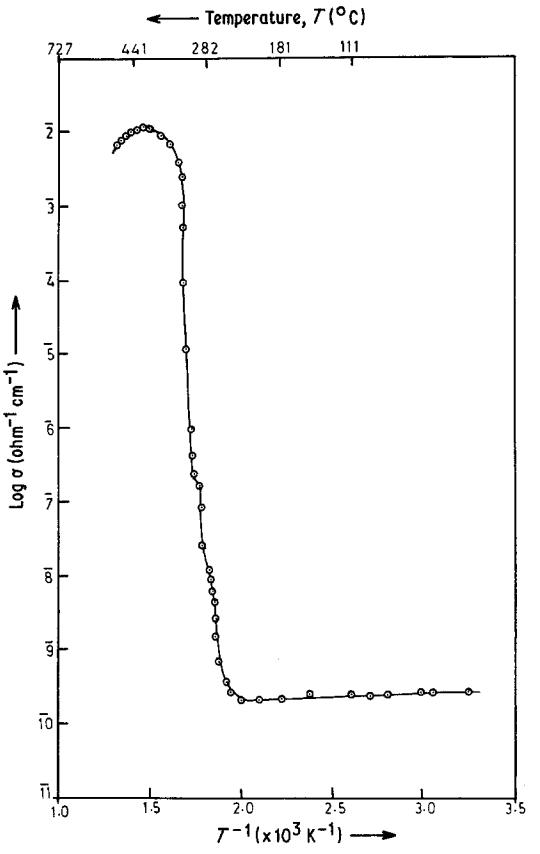

Figure 3 Plot of log σ against T^{-1} of $FeC_2O_4 \cdot 2H_2O$ during decomposition in dynamic air.

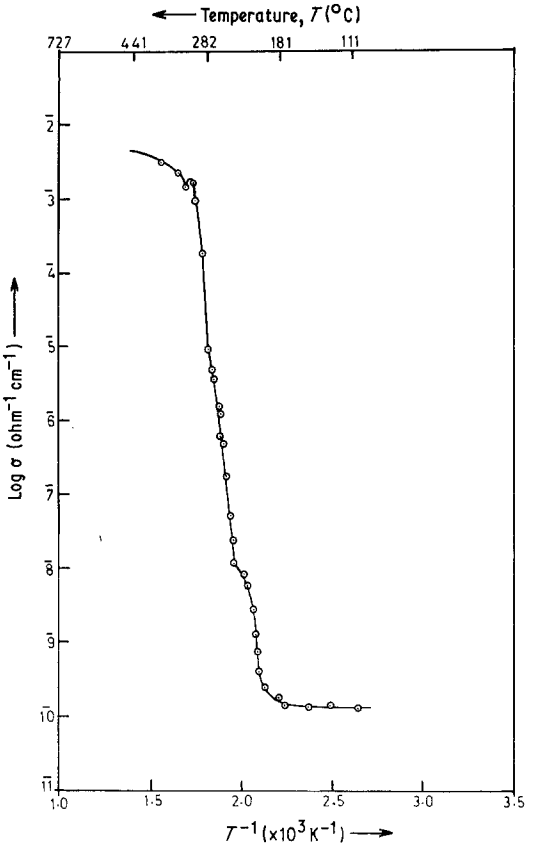

Figure 4 Plot of log σ against T^{-1} of $FeC_2O_4 \cdot 2H_2O$ during decomposition in dynamic air containing water vapour.

defects and subsequent annealing-out of such defects. It is therefore necessary to supplment the electrical conductivity measurements with other measurements of the structural characteristics of the sample, such as measurements of the infrared (i.r.) spectra and of the X-ray diffraction patterns.

At A in Fig. 1 there was little change in σ (Fig. 1). There was also no observable change in the X-ray diffraction pattern and i.r. spectra obtained for this region. The i.r. bands characteristic of the co-ordinated oxalate group [6, 7] observed at 1600(s) (this band is broad due to the overlap of the H_2O band), 1350(m), 1310(m), 815(s),488(m) cm^{-1} were persistent for samples heated up to 160° C. In addition, the bands due to co-ordinated water were observed (see below). The elemental analysis compared well with the formula $FeC_2O_4 \cdot 2H_2O$.

In the temperature range corresponding to Region B in Fig. 1, the i.r. spectra showed large changes. The i.r. spectra of a sample heated at 170° C did not show any bands corresponding to the oxalate group. Bands due to water molecules were observed at 3400(s), 1660(s) and 440(m) cm^{-1}. It should be noted here that the i.r. spectra of samples heated up to 160° C showed bands at 3340(s), 1640(s), 725(m), 580(m), 535(m) cm^{-1}. A comparison of these two i.r. spectra clearly shows that the spectra of a sample heated at 170° C did not show any absorption at 725 cm^{-1} characteristic of co-ordinated water [8–10], such as was observed for a sample heated to 160° C. These results suggest that the water molecules in a sample in the temperature range from room temperature to 160° C are co-ordinated water molecules, while those in a sample heated at 170° C are the lattice water molecules [11, 12]. In addition to the water bands, a strong and broad band at 550 cm^{-1} has been observed for a sample heated at 170° C. This band may be tentatively assigned to Fe–O stretching mode in iron oxide [13]. The sample heated at 170° C shows a complex X-ray diffraction pattern: probably a mixture of FeO, Fe_3O_4 and γ-Fe_2O_3. Thus a

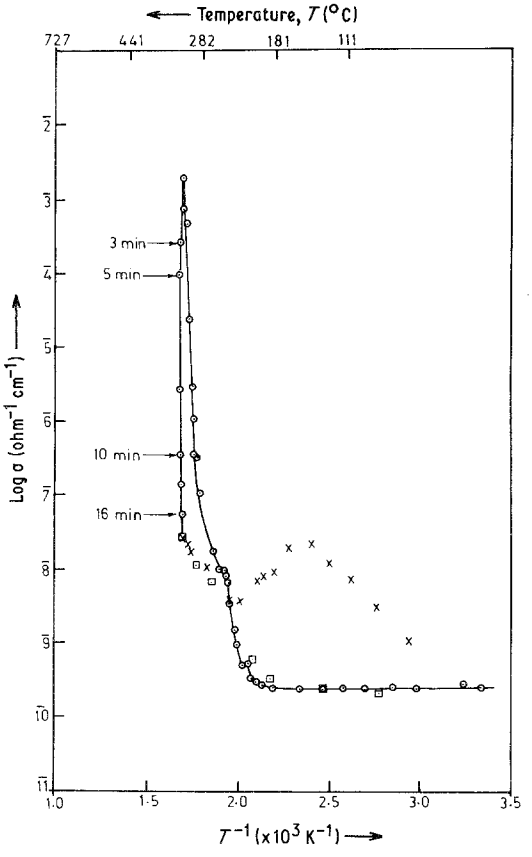

Figure 5 Plot of log σ against T^{-1} of $FeC_2O_4 \cdot 2H_2O$ during decomposition in dynamic air containing water vapour. ⊙ During decomposition; ⊡ cooling cycle for γ-Fe_2O_3; × heating cycle for γ-Fe_2O_3.

steady increase in conductivity observed in Region B in Fig. 1 was due to the transformation of $FeC_2O_4 \cdot 2H_2O$ to metallic Fe_3O_4 possibly through the semiconducting FeO. In this experiment a separate step for the formation of FeO could not be identified. It should be noted here that the conductivity measurements were made on a dynamic system, while the other data were taken on samples obtained by isothermal heating at a specified temperature.

Although a tendencey for a sharp increase in σ was observed at 180° C, the characteristic high σ value of Fe_3O_4 (of about 10^{-3} ohm^{-1} cm^{-1}) could not be obtained under dynamic conditions, and a decrease in σ was seen at 247° C (D in Fig. 1) probably due to the formation of semiconducting γ-Fe_2O_3. A sample in Region C in Fig. 1 was probably a mixture of Fe_3O_4 and γ-Fe_2O_3; the X-ray diffraction pattern was generally broad. From i.r. spectra the lattice water was seen to persist up to 280° C; above this temperature the water bands, if present at all, were very weak.

The temperature range of Regions E′, E″ (Region E in Fig. 1) is very narrow. This part was followed by a region corresponding to the transformation of γ-Fe_2O_3 to α-Fe_2O_3. X-ray diffraction pattern of a sample obtained from Region E shows that it was of predominantly γ-Fe_2O_3 containing a small impurity of α-Fe_2O_3. Thus the conductivity measurements, supplemented with i.r. spectra data, X-ray diffraction pattern data and an elemental analysis, gave a detailed analysis of the thermal decomposition of $FeC_2O_4 \cdot 2H_2O$. The group frequencies of lattice water were persistent up to 280° C. It, therefore, seems that the lattice water plays an important role in the solid-state reaction.

When the reaction has been carried out using the normal atmosphere, the gaseous products acts as a gas buffer for the solid-state reaction and some of the reactions will be ill-defined. For example, the role of co-ordinated water molecules in $FeC_2O_4 \cdot 2H_2O$ and the role of atmospheric oxygen in the solid-state reaction carried out in static air can be clarified by comparing the data of different physical properties for the reaction carried out in a dynamic dry nitrogen atmosphere. I.r. spectra of samples heated at different temperatures give the decisive results. There is no observable change in i.r. spectra up to 90° C. A sample heated at 110° C shows an additional band at 795 cm^{-1}, and its intensity increases with increase of temperature with a corresponding decrease in intensity of the band at 815 cm^{-1} (see Fig. 6). At 210° C the band at 815 cm^{-1} has disappeared completely and the band at 795 cm^{-1} becomes strong and narrow. Other bands of oxalate group observed for the parent compound also show a shift: the 488 cm^{-1} band shows a shift of + 10 cm^{-1}, the 1310 cm^{-1} band shows a shift of + 6 cm^{-1}, the 1350 cm^{-1} band shows a shift of + 10 cm^{-1}, and the 1600 cm^{-1} band shows a shift of about + 40 cm^{-1} (the shift in the 1600 cm^{-1} band cannot be given accurately since the width of this band is about 60 cm^{-1} in aquo complex). The comparison of the group frequencies of water molecules indicates that the sample heated at 210° C does not contain any water molecules, and the change in the nature of bound water (probably co-ordinate water → lattice water) commences at 110° C. Thus Region B (145 to 220° C) of the log σ–T^{-1} plot in Fig. 2 is associated with the dehydration of oxalate. This step includes the transformation of co-ordinated water to lattice

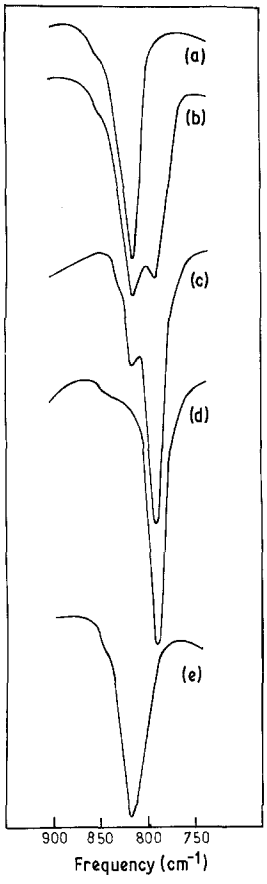

Figure 6 Infra-red spectra of ferrous oxalate in the region 900 to 750 cm^{-1} after equilibrating at different temperatures, T, and then brought to room temperature in the nitrogen atmoshpere. (a) t = room temperature; (b) t = 110° C. (c) t = 150° C; (d) t = 210° C. (e) sample treated as (d) but exposed to water vapour at room temperature for 40 h.

water. Such a transformation is probably associated with the change of octahedral geometry of iron (II) to a tetrahedral one. The colour of the compound changes from the original yellow at room temperature to brown at 210° C. The elemental and oxalate group analyses supplement these results indicating that the sample obtained at 210° C is predominately composed of anhydrous oxalate complex. To confirm these results the sample heated at 210° C was exposed to water vapour in a desiccator at room temperature. I.r. spectra taken at different time intervals show that about 40 h are required to convert FeC_2O_4 to $FeC_2O_4 \cdot 2H_2O$ (Curve e, Fig. 6). A comparison of results obtained in normal static air and in dry nitrogen atmosphere indicates that anhydrous oxalate is obtained only in dry nitrogen atmosphere; in normal static air oxalate is oxidized at much lower temperature. The TG studies performed in a dry nitrogen atmosphere show a small but distinct kink at 210° C corresponding to the dehydration reaction in nitrogen; such a kink is not shown in a similar study conducted in air [1].

The elemental and oxalate analysis and i.r. spectra studies, conducted in a dry nitrogen atmosphere show that oxalate is present in Region C (220 to 347° C) of the log σ against T^{-1} curve (see Fig. 2). The sample heated at 300° C contains 22 wt% oxalate group (anhydrous FeC_2O_2 contains 61.2 wt% oxalate). Estimations of iron content (iron found, 62.2 wt%) indicates that this compound is possibly a mixture of FeC_2O_4 and FeO. X-ray diffraction pattern data obtained in a dry nitrogen atmosphere (Table I) show sharp lines indicating that the sample is predominately crystalline. The pattern fits with the reported data of anhydrous ferrous oxalate [14] and cubic ferrous oxide [15]. Both the X-ray diffraction pattern data and magnetic properties indicate that the above sample does not contain any Fe_3O_4 or Fe metal.

X-ray diffraction pattern data of a sample in a dry nitrogen atmosphere obtained at 425° C show sharp lines and are comparable with the data in [17] reported for Fe_3O_4 (Table II). No line which could be assigned to metallic iron was detected in our work. A steep increase in σ from 10^{-9} ohm^{-1} cm^{-1} to 10^{-3} ohm^{-1} cm^{-1} has been observed at 350° C (Region D in Fig. 2, 350 to 400° C). The sample thus obtained at 425° C shows a negligible variation in σ with variation of temperature. This behaviour is a characteristic of Fe_3O_4 [18–20]. Thus, the X-ray diffraction pattern, the temperature independence of σ, and the magnetic properties (saturation magnetization, 9.0 T kg^{-1}) suggest that the product obtained by thermal decomposition of $FeC_2O_4 \cdot 2H_2O$ under the dynamic nitrogen atmosphere at 425° C is pure Fe_3O_4, and that the concentration of Fe metal, if present at all, is beyond the detection limit of these techniques.

Comparison of the solid-state thermal decomposition reaction of $FeC_2O_4 \cdot 2H_2O$ in normal static air and in dynamic dry nitrogen show the following main differences:

(a) Water molecules remain in the compound up to 280° C in static air, and up to 210° C in dynamic dry nitrogen;

(b) Oxalate is stable up to 170° C in static air and it is stable up to 210° C, and is intimately

TABLE I X-ray diffraction data of FeC_2O_4 and FeO obtained from $FeC_2O_4 \cdot 2H_2O$ by heating under a nitrogen atmosphere at 300° C.

Observed *d*-spacing values (present study) (Å)	FeC_2O_4 *d*-spacing values [14] (Å)	FeO (cubic) *d*-spacing values [15] (Å)	FeO (rhombohedron) *d*-spacing values [16] (Å)
5.16 (s)	5.2 (90)*		
3.95 (s)	3.95 (100)		
2.86 (m)	2.85 (40)		
2.50 (s)		2.49 (80)*	
2.40 (s)	2.40 (90)		
2.32 (m)	2.34 (20)		
2.153 (s)		2.153 (100)	
2.083 (m)	2.10 (30)		
1.945 (m)	1.93 (50)		
1.881 (w)	1.88 (20)		
1.833 (m)	1.83 (50)		
1.763 (m)	1.755 (40)		
1.711 (w)	1.715 (20)		
1.692 (m)	1.695 (30)		
1.520 (m)		1.523 (60)	1.525 (100)*
			1.512 (100)
1.300 (w)		1.299 (25)	1.301 (20)
			1.236 (60)
1.077 (w)		1.077 (15)	1.074 (60)

*Figures in parenthesis show the relative line intensities, normalized to that of the strongest intensity line (given by 100).

associated with the decomposed product, up to 350° C in dry nitrogen.

The nature of the final product depends on these two main differences. Since the solid-state thermal decomposition of $FeC_2O_4 \cdot 2H_2O$ is influenced by the composition of the atmosphere, it would be advantageous to undertake similar measurements in other controlled atmospheres.

I.r. spectra of ferrous oxalate heated in dynamic dry air suggest that it is stable up to 230° C. Water molecules remain in the sample up to 280° C in this atmosphere. There is a steep increase in σ at 240° C followed by another steep increase at 288° C (see Fig. 3). These two temperature ranges 240 to 290° C and 290 to 320° C are tentatively assigned to the formation of FeO and Fe_3O_4, respectively. However, our repeated experiments to obtain pure FeO by careful heating in dynamic air, even at 245° C, always led to the formation of a mixture of FeO and Fe_3O_4 (see Table III) [15–17]. Since the X-ray diffraction pattern of the sample thus obtained displays broad lines, the product seems to be less crystalline. The lines assigned to FeO fit with the cubic structure. It should be noted here that the sample consisting of anhydrous FeC_2O_4 and FeO during the solid-state reaction under a dry nitrogen atmosphere contains both these constituents in highly crystalline form. A pure sample of Fe_3O_4 has been obtained by heating a sample at 300° C. A broad maximum in log σ against T^{-1} curve has been observed between 320 and 402° C. The conductivity measurements on the oxide thus obtained at 402° C on cooling and reheating indicate the formation of α-Fe_2O_3. X-ray diffraction pattern analysis has confirmed the formation of this phase. The temperature at which Fe_3O_4 is converted to α-Fe_2O_3 in dynamic air (402° C) is much higher than that in static air (330° C). In addition, the steps corresponding to the dehydration of oxalate, and the transformation of Fe_3O_4 to γ-Fe_2O_3 could not be differentiated in dynamic air. These observations suggest that the solid-state decomposition of $FeC_2O_4 \cdot 2H_2O$ under the buffer atmosphere in static air and in dynamic air follow different routes. Experimental data determined in dynamic air containing water vapour would provide further information on the solid-state thermal decomposition of $FeC_2O_4 \cdot 2H_2O$.

The progress of decomposition of $FeC_2O_4 \cdot 2H_2O$ in dynamic air containing water vapour, as studied by i.r. spectra, indicates that the oxalate is stable up to 190° C and water bands persist up to 280° C. There is a steep increase in σ at 190° C followed by another steep increase at 250° C (see Fig. 4). Comparison of σ curves obtained in dynamic air and obtained in dynamic air containing water vapour indicates that the pattern of decom-

TABLE II X-ray diffraction data of Fe_3O_4 obtained from $FeC_2O_4 \cdot 2H_2O$ by heating under nitrogen atmosphere at 425° C.

Observed *d*-spacing values (present study) (Å)	Fe_3O_4 *d*-spacing values [17] (Å)
4.86 (w)	4.85 (8)*
2.965 (m)	2.967 (30)
2.530 (s)	2.532 (100)
2.421 (w)	2.424 (8)
2.093 (m)	2.099 (20)
1.705 (w)	1.715 (10)
1.609 (m)	1.616 (30)
1.478 (m)	1.485 (40)
	1.419 (2)
	1.328 (4)
1.275 (w)	1.281 (10)
	1.266 (4)
	1.212 (2)
	1.122 (4)
1.091 (w)	1.093 (12)
1.048 (w)	1.050 (6)
	0.9896 (2)
0.967 (w)	0.9695 (6)
	0.9635 (4)
	0.9388 (4)
	0.8952 (2)
0.880 (w)	0.8802 (6)
0.853 (w)	0.8569 (8)
	0.8233 (4)
0.812 (w)	0.8117 (6)
	0.8080 (4)

*Figures in parentheses show the relative line intensities, normalized to that of the strongest intensity line (given by 100).

position is not very different for the two environments. Temperatures for the formation of FeO and Fe_3O_4 are compartively low in dynamic air containing water vapour. In addition, a definite well-resolved kink in the log $\sigma - T^{-1}$ plot has been observed between 300 and 318° C in dynamic air + water vapour (see Fig. 4). A careful analysis of the time-dependent σ measurements in this temperature range shows the following points:

(a) There is no change in σ with time up to 314° C;

(b) At 314° C the specific conductivity changes from 10^{-3} ohm^{-1} cm^{-1} to 10^{-8} ohm^{-1} cm^{-1} within 16 min (see Fig. 5);

(c) There is no further decrease in σ above 314° C;

(d) For a sample heated to 314° C and then cooled, the log σ against T^{-1} curves for cooling and heating do not overlap and, while the cooling curve is reasonably linear with a negative slope, the heating curve shows a definite maximum (see Fig. 5).

The sample thus obtained was heated under nitrogen at 300° C to remove any water. The X-ray diffraction pattern of this sample is sharp and the sample seems to be highly crystalline. Its X-ray diffraction pattern is similar to that reported for the tetragonal γ-Fe_2O_3 [21]; the relative intensities for the *d*-spacing values of 2.78, 2.638, 1.820 and 1.604 Å (see Table IV) are characteristically different for the tetragonal and cubic structures [21, 22].

A systematic comparitive study of the X-ray diffraction patterns of γ-Fe_2O_3 obtained by various methods has been reported [23]. The analysis is mainly based on the presence of the (200) line (assigned relative intensity of 1) for the cubic configuration; this line is absent for the tetragonal configuration. Other lines which are considered for the comparative study are the (110), (210), (211) lines of the cubic configuration,

TABLE III X-ray diffraction data of Fe_3O_4 and FeO obtained from $FeC_2O_4 \cdot 2H_2O$ by heating under dynamic air at 245° C

Observed *d*-spacing values (present study) (Å)	Fe_3O_4 *d*-spacing values [17] (Å)	FeO (cubic) *d*-spacing values [15] (Å)	FeO (rhombohedron) *d*-spacing values [16] (Å)
2.984 (m)	2.967 (30)*		
2.532 (s)	2.532 (100)		
2.485 (s)		2.49 (80)*	
2.155 (s)		2.153 (100)	
2.088 (w)	2.099 (20)		
1.595 (m)	1.616 (30)		1.525 (100)*
			1.512 (100)
1.523 (m)		1.523 (60)	
1.486 (m)	1.485 (40)		
1.300 (w)		1.299 (25)	1.301 (20)

*Figures in parentheses show the relative line intensities, normalized to that of the strongest intensity line (given by 100).

TABLE IV Related intensities of some X-ray diffraction lines of γ-Fe_2O_3 with tetragonal and cubic structures.

Observed *d*-spacing values of γ-Fe_2O_3 (present study) (Å)	γ-Fe_2O_3 (tetragonal) *d*-spacing values [21] (Å)	γ-Fe_2O_3 (cubic) *d*-spacing values [22] (Å)
2.78 (3)*	2.78 (3)*	2.78 (19)*
2.640 (3)	2.638 (4)	2.64 (–)
2.521 (100)	2.514 (100)	2.52 (100)
1.822 (4)	1.820 (3)	–
1.611 (22)	1.604 (20)	1.61 (33)

*Figures in parentheses show the relative line intensities, normalized to that of the strongest intensity line (given by 100).

which are also shown by the tetragonal configuration; these lines have a correspondence with the $N = 2, 5, 6$ lines of maghemite. The additional lines shown for the tetragonal structure, used for the comparative study, have weak intensities. We consider, therefore, that, in addition to the presence of these additional weak lines, the relative intensities of the lines summarized in Table IV which are characteristically different for the tetragonal and cubic configurations, can be profitably used to differentiate the different structures of γ-Fe_2O_3. The pattern does not even show a weak line corresponding to α-Fe_2O_3 (Table V). The magnetic hysteresis measurements made on this sample show that it has a coercive force, (H_C), of 3.142 A m^{-1} and saturation magnetization of 7.1 T kg^{-1}. These values are comparable with the data given in [1]. Further analysis of the conductivity–temperature behaviour of γ-Fe_2O_3 during cooling and heating cycles is required. α-Fe_2O_3 is formed at 325° C in dynamic air containing water vapour.

Now let us analyse the different paths of the decomposition of $FeC_2O_4 \cdot 2H_2O$ in different atmospheres. A complete dehydration of $FeC_2O_4 \cdot 2H_2O$ has been obtained only under the dynamic dry nitrogen atmosphere, as has been seen from the characteristic shift of the oxalate band at 815 cm^{-1} on dehydration. A transformation of FeC_2O_4 to FeO has been detected. A separate phase of FeO could not be obtained and it always occurs with FeC_2O_4. Thus the transformation of FeC_2O_4 to FeO seems to be an equilibrium reaction. This mixture of FeO and FeC_2O_4 is then transformed to Fe_3O_4 which is a final product obtained in dry nitrogen. These reactions are presented as follows:

TABLE V X-ray diffraction data of γ-Fe_2O_3 obtained from $FeC_2O_4 \cdot 2H_2O$ by heating under dynamic air containing water vapour at 314° C.

Observed *d*-spacing values of γ-Fe_2O_3 (present study) (Å)	γ-Fe_2O_3 (tetragonal) *d*-spacing values [21] (Å)	γ-Fe_2O_3 (cubic) *d*-spacing values [22] (Å)
7.91 (w)	7.91 (1)*	
6.95 (w)	6.94 (2)	
5.90 (w)	5.90 (6)	5.90 (2)*
5.34 (w)	5.33 (1)	
4.83 (w)	4.82 (6)	4.82 (5)
4.29 (w)	4.29 (2)	
		4.18 (1)
3.73 (w)	3.73 (6)	3.73 (5)
3.39 (w)	3.40 (7)	3.41 (2)
3.20 (w)	3.20 (3)	
2.95 (m)	2.95 (30)	2.95 (34)
2.78 (w)	2.78 (3)	2.78 (19)
2.640 (w)	2.638 (4)	2.64 (–)
2.517 (s)	2.514 (100)	2.52 (100)
2.405 (w)	2.408 (2)	
2.320 (w)	2.315 (2)	2.32 (6)
2.230 (w)	2.230 (2)	2.23 (1)
2.085 (m)	2.086 (15)	2.08 (24)
1.863 (w)	1.865 (1)	1.87 (4)
1.822 (w)	1.820 (3)	
1.691 (m)	1.701 (19)	1.70 (12)
1.668 (w)	1.670 (2)	
1.611 (m)	1.604 (20)	1.61 (33)
1.545 (w)	1.550 (2)	1.55 (< 1)
1.525 (w)	1.525 (3)	1.53 (1)
1.476 (m)	1.474 (40)	1.48 (53)
1.314 (w)	1.318 (6)	1.32 (7)
1.274 (w)	1.272 (8)	1.27 (11)
1.257 (w)	1.258 (3)	1.26 (3)
1.194 (w)	1.204 (5)	1.21 (5)
1.112 (w)	1.115 (6)	1.12 (7)
1.084 (w)	1.086 (10)	1.09 (19)
		1.07 (1)
1.040 (w)	1.043 (7)	1.04 (8)
		1.04 (1)
		1.03 (1)
0.981 (w)	0.983 (5)	
0.960 (w)	0.963 (8)	
0.930 (w)	0.932 (4)	

*Figures in parentheses show the relative line intensities, normalized to that of the strongest intensity line (given by 100).

$$FeC_2O_4 \cdot 2H_2O \xrightarrow{145–220^\circ C} FeC_2O_4 + 2H_2O\uparrow; \quad (1)$$

$$FeC_2O_4 \xrightarrow{220–350^\circ C} FeO + CO\uparrow + CO_2\uparrow; \quad (2)$$

$$2FeO + FeC_2O_4 \xrightarrow{350–400^\circ C} Fe_3O_4 + 2CO\uparrow. \quad (3)$$

There are inconsistencies in the reported TG data of $FeC_2O_4 \cdot 2H_2O$ in dry nitrogen. According to [1] the total mass loss up to 270° C was 60 wt%, and was assigned to the formation of FeO; the source of oxygen in the formation of Fe_3O_4 from FeO in dry nitrogen was not given. According to [3] the total mass loss was reported to be 57 wt%, and was assigned to the formation of Fe_3O_4.

In dynamic air, the decomposition of oxalate takes place prior to dehydration. The decomposed product has been shown to be a mixture of FeO and Fe_3O_4. A separate step for its further decomposition to Fe_3O_4 has been obtained. Both FeO and Fe_3O_4 contain lattice water. The final step is the decomposition of Fe_3O_4 to α-Fe_2O_3. The probable formation of γ-Fe_2O_3 as an intermediate step is not detected. The final step probably involves the reaction with atmospheric oxygen. (The exact stoichiometry of these reactions could not be determined.)

$$FeC_2O_4 \cdot 2H_2O \xrightarrow{240^\circ C} FeO \cdot xH_2O + Fe_3O_4 \cdot yH_2O + CO\uparrow + CO_2\uparrow; \quad (4)$$

$$FeO \cdot xH_2O + Fe_3O_4 \cdot yH_2O \xrightarrow{290^\circ C} Fe_3O_4 \cdot zH_2O; \quad (5)$$

$$Fe_3O_4 \cdot zH_2O \xrightarrow{290\text{–}320^\circ C} Fe_3O_4 + H_2O; \quad (6)$$

$$Fe_3O_4 + O_2 \xrightarrow{402^\circ C} \alpha\text{-}Fe_2O_3. \quad (7)$$

In dynamic air containing water vapour the decomposition path is similar to that in dynamic dry air except for the step represented by Equation 7. Our experimental data suggest that water vapour plays an important role in this final step. As the partial pressure of water used in this experiment is much higher than that used in dry air (in which case the partial pressure will be due only to the lattice water), lattice water is possibly not removed, during the decomposition of $Fe_3O_4 \cdot zH_2O$, only in for form of water molecules; it may be decomposing to oxygen and hydrogen. Under these conditions the intimately associated oxygen would be responsible for the clear observation of the step corresponding to the formation of γ-Fe_2O_3 (the exact stoichiometries are not shown):

$$Fe_3O_4 \cdot zH_2O \xrightarrow{250\text{–}300^\circ C} Fe_3O_4 \cdot [O] \cdot wH_2O + H_2; \quad (8)$$

$$Fe_3O_4 \cdot [O] \cdot wH_2O \xrightarrow{314^\circ C} \gamma\text{-}Fe_2O_3 + [O]; \quad (9)$$

$$\gamma\text{-}Fe_2O_3 \xrightarrow{\text{above } 325^\circ C} \alpha\text{-}Fe_2O_3. \quad (10)$$

In static air the reaction pattern is similar to that in dynamic air containing water vapour. The gaseous products of the decomposition reaction act as a gas buffer for the solid-state reaction. In fact, it has been suggested that to arbitrarily add a few drops of water to $FeC_2O_4 \cdot 2H_2O$ during decomposition in static air [1] will promote the formation of γ-Fe_2O_3. It should be noted here that γ-Fe_2O_3 obtained in static air is always contaminated with α-Fe_2O_3. It may be due in part to the participation of atmospheric oxygen during the decomposition of Fe_3O_4 since the partial pressure of water may not be sufficient to have a well separated reaction represented by Equation 9.

4. Conclusions

The present study suggests the following important points in the solid-state decomposition of $FeC_2O_4 \cdot 2H_2O$.

(a) The dehydration of $FeC_2O_4 \cdot 2H_2O$ yielding anhydrous FeC_2O_4 takes place only in dry nitrogen. In other atmospheres, oxalate decomposes prior dehydration.

(b) Water persists with the decomposed compound up to a temperature of 280° C in a static normal atmosphere, dry dynamic air, and dynamic air containing water vapour.

(c) In dry nitrogen the log σ against T^{-1} plot shows a well-characterized step corresponding to dehydration. The formation of FeO as an intermediate product in the formation of Fe_3O_4 is confirmed; FeO is always formed together with FeC_2O_4.

(d) Although the electrical conductivity measurements indicate a separate step for the formation of FeO in dynamic air, and in dynamic air containing water vapour, FeO in the pure state could not prepared.

(e) The electrical conductivity measurements give a separate step for the formation of Fe_3O_4 in dynamic air, and dynamic air containing water vapour. Fe_3O_4 has been separated in the pure state using both of these atmospheres. In a dry nitrogen atmosphere, the reaction does not proceed beyond Fe_3O_4.

(f) The formation of γ-Fe_2O_3 prior to the

formation of α-Fe_2O_3 could not be detected in dry dynamic air from electrical conductivity measurements. In dynamic air containing water vapour the formation of γ-Fe_2O_3 has been clearly shown. The exact conditions, determined by electrical conductivity measurements for obtaining γ-Fe_2O_3 in dynamic air containing water vapour (obtained by passing air through temperature-controlled water at 60 to 61° C) are: air flow, 60 to 65 ml min^{-1}; temperature, 314° C; time, 16 min.

(g) γ-Fe_2O_3 thus obtained does not contain any traces of α-Fe_2O_3. It has the desired magnetic properties: coercive force, 3.142 A m^{-1}, saturation magnetization, 7.1 T kg^{-1}; ratio of remanence to saturation magnetization, 0.64.

(h) The solid-state reaction in static air of $FeC_2O_4 \cdot 2H_2O$ seems to be complex.

(i) The TG, DTG, and DTA results taken in dry nitrogen show dehydration and the overall decomposition reaction. These measurements do not give any indication of the different intermediate products formed. The d.c. electrical conductivity measurements supplemented with i.r. spectra investigations and X-ray diffraction studies have clearly indicated the steps corresponding to the formation of various intermediate products.

Acknowledgements

This work has been undertaken with financial support from Khosla Research Project. A senior fellowship (KSR) and a junior fellowship (AKN) have been awarded. Our thanks are due to the late Professor A. B. Biswas, Indian Institute of Technology, Bombay, India, for the facilities given for the part of the work.

References

1. V. RAO., A. L. SHASHIMOHAN and A. B. BISWAS, *J. Mater. Sci.* 9 (1974) 430.
2. S. C. BEVAN and R. A. BROWN, *J. Inorg. Nucl. Chem.* 28 (1966) 387.
3. D. BROADBENT, J. DOLLIMORE and D. DOLLIMORE, *J. Chem. Soc. A* (1967) 451.
4. J. TRAU, *J. Thermal Anal.* 6 (1974) 355.
5. S. D. LIKHITE, C. RADHAKRISHNAMURTHY and P. W. SAHASRABUDHE, *Rev. Sci. Instrum.* 36 (1965) 1558.
6. J. FUJITA, A. E. MARTELL and K. NAKAMOTO, *J. Chem. Phys.* 36 (1962) 324.
7. *Idem, ibid.* 36 (1962) 331.
8. J. FUJITA, K. NAKAMOTO and M. KOBAYASHI, *J. Amer. Chem. Soc.* 78 (1956) 3963.
9. I. GAMA, *Bull. Chem. Soc. Japan* 34 (1961) 760.
10. *Idem, ibid.* 34 (1961) 1430.
11. P. J. LUCCHEST and W. A. GLASSON, *J. Amer. Chem. Soc.* 78 (1956) 1347.
12. J. van der ELSKEN and D. W. ROBINSON, *Spectrochim. Acta* 17 (1961) 1249.
13. N. T. McDEVITT and W. L. BAUN, *ibid.* 20 (1964) 799.
14. ASTM File number 14–807.
15. ASTM File number 6–615.
16. ASTM File number 6–711.
17. ASTM File number 19–629.
18. C. A. DOMENICALI, *Phys. Rev.* 78 (1950) 458.
19. B. A. CALHOUN, *Phys. Rev.* 94 (1954) 1577.
20. P. A. MILES, W. B. WESTPHAL and A. VON HIPPEL, *Rev. Mod. Phys.* 29 (1957) 279.
21. ASTM File number 25–1402.
22. ASTM File number 24–81.
23. J. D. BERNAL, D. R. DASGUPTA and A. L. MACKAY, *Clay Mineral Bull.* 4 (1959) 15.

Received 22 May 1980 and accepted 11 February 1981.